Bubble Formation and Detachment in Liquid Flow Under Normal and Reduced Gravity

Henry K. Nahra
Lewis Research Center, Cleveland, Ohio

Y. Kamotani
Case Western Reserve University, Cleveland, Ohio

National Aeronautics and
Space Administration

Lewis Research Center

January 1998

Available from

Bubble Formation and Detachment in Liquid Flow Under Normal and Reduced Gravity

Henry K. Nahra
Microgravity Fluid Physics Branch
Microgravity Science Division
NASA-LeRC

Cleveland, OH

Y. Kamotani
Department of Mechanical & Aerospace
Engineering
Case Western Reserve University

Cleveland, OH

1. Abstract

Two-phase flows are present in a wide variety of applications for spacecraft thermal control systems design. Bubble formation and detachment is an integral part of the two-phase flow science. The authors[1] objective is to experimentally investigate the effects of liquid cross velocity, gas velocity, and nozzle diameter on the bubble diameter at detachment under reduced and normal gravity and under relatively low gas flow rates. Results from ground (1 g) and reduced gravity experiments will be presented in this paper. For the 1g experiment, a flow loop was designed and built to accommodate a range of liquid and gas flow rates. The reduced gravity experiment was conducted on the NASA DC-9 reduced gravity platform using the two-phase flow loop qualified for operation on the low-gravity platform. Flow visualization is accomplished using a high speed 500 frames/s camera. The results suggest that the existence of buoyancy force contributes to the faster detachment of bubbles. Buoyancy helps the detachment process which results in smaller bubbles being formed. In reduced gravity, although drag force is present, the virtual non-existence of buoyant force results in larger bubbles and longer times for detachment. Theoretical predictions are also presented in this paper and seem to agree with the experimental results.

2. Introduction

The power requirements for current and future space missions are increasing due to rising power demand. More efficient and larger capacity thermal control systems for space applications are, therefore, needed to handle the increasing power requirements. Two-phase flow thermal control systems provide more effective thermal transport in spacecrafts[1] due to the higher latent heat of vaporization of fluids when compared to their sensible heat. Two-phase flow phenomena are encountered in space propulsion systems, thermal control of power generation and distribution subsystems, cryogenic liquid transfer and storage systems, life support systems, and systems related to commercial development of space programs[2,3].

Dispersed phase bubble or droplet formation and behavior play an important role in two phase flows. Understanding of such a behavior in microgravity is crucial because of its direct implications to the design of two phase flow systems for large space structure such as the space station.

Understanding the behavior of dispersed bubble in microgravity includes the understanding of bubble formation, its growth, shape, detachment and the forces involved in affecting these processes. Due to the virtual absence of the buoyancy force, detachment of bubbles is very different under microgravity especially at low gas flow rates. One method to help detach forming bubbles is to apply a cross flow where the drag force helps the bubble detachment[3]. The purpose of this work is to experimentally investigate the effects of liquid cross velocity, gas velocity, and nozzle diameter on the bubble diameter at detachment under reduced and normal gravity.

3. Experimental

3.1 Ground Flow Loop

The ground (1 g) flow loop was built in order to perform the Bubble Formation and Detachment in a Liquid Cross Flow experiment. A schematic is shown in Figure 1. A centrifugal pump was used to establish the liquid flow in a square 2.54 cm (1") hydraulic diameter channel. The liquid flow rate was measured with two liquid flow meter connected in parallel and used depending on the liquid flow rates which ranged from 0 to 6000 ml/min. The gas flow rate was at first established from a pressurized air bottle. However, due to the need to establish low liquid air flow rates, a syringe pump was used. The latter established the desired/calibrated rates up to 13 ml/min. The flow channel was constructed from Plexiglass® and pressure tested to 2.58 10^6 dynes/cm^2 (37.5 psi) with no water leaks observed. A bypass loop was also established in order to have better control on the liquid flow rates. The liquid is pumped into the channel and its flow rate is controlled. The syringe pump is then turned on and allowed to run until sufficient pressure is built in the syringe in order to prevent any liquid back-flow into the syringe. Then a gate valve is open to allow the air into the liquid cross flow. Two orifice diameters (.033 cm and .076 cm) were used (one at the time) for air injection into the liquid flow. The orifices were flush with the plexiglass surfaces in order to reduce flow disturbances. The .033 cm orifice design resembled a converging nozzle whereas the design of the .076 cm orifice resembled a tube with an inner diameter of .076 cm. Figure 2 shows a schematic of the two nozzle designs used in the 1g and low g experiments. A high-speed camera (nac 500 or nac 1000) is used to videotape the events of bubble generation and detachment.

3.2 Low-Gravity Two-Phase Flow Loop

This flow loop is frequently used for two phase flow experiments requiring low gravity[6]. It consists of a liquid flow subsystem which is composed of a water reservoir made of Plexiglass® and fitted with a piston which is driven by air pressure provided by air bottle on board of the DC-9 platform. The loop has a gas flow subsystem which provides the gas flow into the liquid in order to establish the various regimes of two-phase flows. Since the existing gas flow system could not accommodate the required low gas flow rates, it was decided to integrate the syringe pump to establish the gas flow rates. The same flow

channel was integrated into the loop. The same two orifices/injectors (of diameters .033 and .076 cm) were used to generate the air bubbles in the cross flow. Data acquisition is furnished by the two phase flow loop as well. Liquid and gas flow rates as well as acceleration data is written to files in binary format. Flow visualization is accomplished using the same high speed cameras used in the 1 g ground experiments. Figure 3 shows the arrangement flown on board of the DC-9 low gravity platform.

4. Experimental procedure and Data Analysis

The procedure for the ground experiment is similar to the one applied in the low gravity environment. The liquid flow is first established, then air is introduced through the orifice nozzle. Several liquid flow rates are accomplished with several gas flow rates for each of the orifices. The recorded video data was analyzed using the *TRACKER* software[4] commonly used at *NASA*. This enabled the measurement of the bubble diameter at or very near the detachment point. The measurement is based on a count of pixels and a comparison with an existing scale. These measurements, in addition to Time to Detachment *(TTD)* measurements were entered in a text/data file. The data file was read by a MATHEMATICA®™ program which calculated the bubble average diameter, the standard deviation of the mean and the mean *TTD* designated by *MTTD*.

5. Prediction of Bubble Diameter at Detachment

5.1 Governing Equations

Prediction of the detachment bubble diameter is accomplished using a force balance on the bubble as it is forming from the nozzle. The coordinate system used in this calculation is illustrated in Figure 4. The force balance is given by the following

$$\frac{d}{dt}\left(M_b \frac{d\bar{S}}{dt}\right) = \sum_{j=1}^{n} \bar{F}_j \qquad (1)$$

where $\bar{S}$ is the position vector of the bubble center of mass, M_b is the bubble mass and $\bar{F}_j$ is the jth force acting on the bubble. The forces acting on the bubble are the drag, the surface tension, the rate of momentum from the gas flow, and the buoyancy forces. The term on the left hand side

of (1) is defined as the inertia term. The forces are given respectively by the following equations[3,5]

$$F_{Di} = \tfrac{1}{2} C_D \rho_c A U U_i \qquad (2)$$

$$F_{Si} = \pi \sigma D_N f(\phi)_i \qquad (3)$$

$$F_M = \rho_d \frac{4 Q_d^2}{\pi D_N^2} \qquad (4)$$

$$F_B = (\rho_c - \rho_d) V_b g \qquad (5)$$

where the subscripts c and d designate the continuous and dispersed phases respectively, the subscripts B and b designate the buoyancy and bubble, the subscript i designates the ith direction (x, y or z) in Cartesian coordinates, C_D is the drag coefficient, A is the effective area, U is the relative velocity, D_N is the nozzle diameter, $f(\phi)_i$ is the surface tension function that changes with the bubble inclination ϕ (as shown in Figure 4) and which depends on the Cartesian coordinates, Q_d is the gas flow rate, and V_b is the bubble volume. The last two forces (4) and (5) point in the direction +y opposite to the direction of g which is defined in this calculation as -y. The direction of the cross flow velocity U_{Ls} is defined as +x direction. Equation (1) is decomposed into its components which are $X(t)$, $Y(t)$, and $Z(t)$. Since the bubble mass M_b is changing with time, an added mass coefficient[3] results from the expansion and the displacement of the surrounding fluid. In this calculation, an added mass coefficient[7] $C_M = \tfrac{11}{16}$ was used in the inertial terms of the equation of motion. The non-linear ordinary second order coupled differential equations for the expansion and detachment phases were solved using the *NDSOLVE* routine in *MATHEMATICA*®™.

5.2 Expansion Phase
Two phases are identified in the process of bubble formation. The first is the expansion phase whose end is defined by the minimum of the times t_x and t_y the first of which satisfies the following criteria,

$$\sqrt{X(t)^2 + Z(t)^2} - \tfrac{1}{2}\left(D_B(t) + D_N\right) \geq 0 \quad (6)$$

and the second of which satisfies the force balance in the y direction. In other words, t_x and t_y are the root solutions of equation 6 and the y direction force balance and the end of the bubble formation phase is given by $t_e = Min[t_x, t_y]$. During this phase, $Y(t)$ was taken to equal $\tfrac{1}{2}D_B(t)$ which can be calculated from a simple expansion process where it is proportional to $t^{1/3}$. The $X(t)$ and $Z(t)$ components are solved simultaneously.

This amounted to solving a system of second order nonlinear ordinary differential equations. After obtaining $X(t)$ and $Z(t)$, criterion (6) and the y direction force balance are checked. If $t_x < t_y$, then the bubble is detached before starting the detachment phase. If $t_y < t_x$, then the upward forces on the bubble are sufficient to lift the bubble which begins developing a neck. This begins the detachment phase.

5.3 Detachment Phase
In this phase the three components of the equation of motion were solve simultaneously. The initial conditions were the same as the conditions at the end of the expansion phase. From the $X(t)$, $Y(t)$ and $Z(t)$ functions, two detachment criteria are evaluated. The first is equation (6) and the second is based on the neck length and is given by[3]

$$\sqrt{X(t)^2 + Y(t)^2 + Z(t)^2} - \left(\tfrac{1}{2} D_B(t) + D_N\right) \geq 0$$
$$(7)$$

After determining the times at which equations (6) and (7) are satisfied, a geometric average of the two times is determined and then used to evaluate the detachment diameter. The drag coefficient which is a function of the bubble Reynolds number is iterated in the solution of both the expansion and detachment phase.

6. Results-Comparison of Predicted and Measured Bubble Diameter at Detachment
The results from the experiments and the analytical predictions are presented in this section for the 1 g and low g environments respectively.

6.1 Full g results
Comparison between analytical predictions and experimental results under full gravity is shown in Figure 5 for $D_N=.033$ cm and $D_N=.076$ cm. From the lower set of data ($D_N=.033$ cm), the % difference between experimental and predicted diameters ranges from 9 to 16%. From the higher set of data ($D_N=.076$ cm), the difference ranges between 4 and 14%. The air flow rate in figure 5 is 8 and 13 ml/min corresponding respectively to $D_N=.033$ and .076 cm. Overall, the prediction compared reasonably well with experimental results under full gravity. The predictions of detachment diameter for superficial velocities less that 4.5 cm/s were not possible due to an instability in the solution. The two aforementioned detachment criteria during the detachment phase have no solutions for $U_{Ls} < \sim 4.5$ cm/s. As a result,

the predicted curve stopped at the data point prior to 4.5 cm/s, i.e. at 5.82 cm/s.

6.2 Low g results

Figure 6 shows the experimental and predicted bubble diameters at detachment for Q_d=8 ml/min, D_N=.033 cm (the lower curve and data) and D_N=.076 cm (the upper curve and data) respectively. From the plotted data of Figure 6, the difference between experiment and prediction ranged from 1 to 13% for D_N=.033 cm and from 4 to 15% for D_N=.076 cm. As under the full gravity, the prediction compared reasonably well with the experimental results.

Figure 7 shows a plot of the predicted Time To Detachment (TTD) vs. U_{LS} for low and full gravity. The predicted TTD is higher under low gravity due to the lack of buoyancy force. It is apparent also that the TTD of the low g case is three times as large as the 1 g case. Figure 8 shows the experimental MTTD and calculated TTD as a function of the cross liquid velocity for Q_d=3.8 ml/min and D_N=.076 cm. The difference between MTTD and TTD ranged from 10 to 18%. Figure 9 shows a comparison of the bubble growth and detachment under 1 g (a) and in low g (b) for Q_c=4000 ml/min, D_N=.033 cm, Q_d=10 ml/min. The traces of the developing bubbles were captured from exactly the same size digitized video images. It is apparent that lack of buoyancy results in larger, more spherical bubbles produced by the .033 cm nozzle.

6.3 Discussion

As shown from the aforementioned results, the agreement between the experimental and calculated detachment bubble diameter was reasonably good. The agreement was better in the low g results than under the full g. Also the agreement between experiment and prediction is better in the high liquid cross velocity than in the lower cross velocity region. From these observations, it can be seen that the model solved here predicts within 10% the bubble detachment diameter for the higher liquid cross velocity region under low g setting. The same statement can be made regarding the 1g setting, however, we should expect slightly larger uncertainty in the bubble detachment diameter.

7. Concluding Remarks

We have shown in this paper the results of ground and low gravity bubble generation and detachment

in a liquid cross flow experiment. We have also shown the results of the prediction of the bubble diameter at detachment which was based on a force balance applied on the evolving bubble. The prediction compared well with the experiment with a difference not exceeding 16 % in all the cases studied.

The same arrangement was flown again, however, on the second flight, a flow meter with a set point was used to control the air flow into the liquid cross flow. This air flow controller provided wider range of flow air rates than the syringe. The data is currently being analyzed using the TRACKER[4] software which was used for the first flight. The same model will eventually be applied to compare the predictions with the experimental results.

References

1. Eastman et.al. "Two phase Fluid Transport for Spacecraft", AFWAL-TR-84-3028.

2. Ostrach S., "Industrial Processes Influenced by Gravity" NASA CR-182140, C-21066-G, 1988.

3. lee-Hwan Kim et.al. "Modeling of Bubble and Drop Formation in Flowing Liquids in Terrestrial and Microgravity Environments," EMAE/TR-92-207, Case Western University, Cleveland, OH, May 1992.

4. Klimek R. B., Wright T. W., Sielken R. S., "Color Image Processing and Object Tracking System", NASA TM-107144, February, 1996.

5. leeHwan Kim et.al. "Modeling of Bubble and Drop Formation in Flowing Liquids in Microgravity," AIChE, Vol. 40, No. 1, 1994.

6. McQuillen, J. B., and Neumann, E. S., "Two-Phase Flow Research Using the Learjet Apparatus", NASA TM-106814, May 1995.

7. Kawase, Y., and Ulbrecht, J. J., "Formation of Drops and Bubbles in Flowing Liquids", Ind. Eng. Chem. Process Des. Dev., 20,636, 1981.
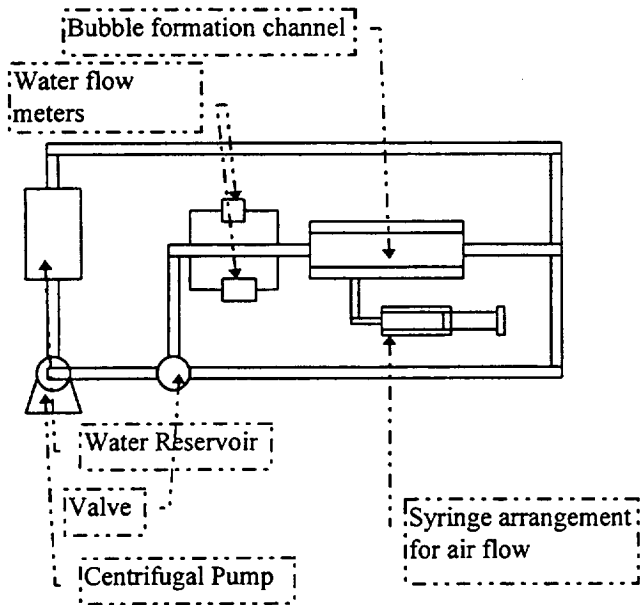
Figure 1. Simplified Schematic of the Ground Flow Loop used for the Bubble Formation and Detachment experiment
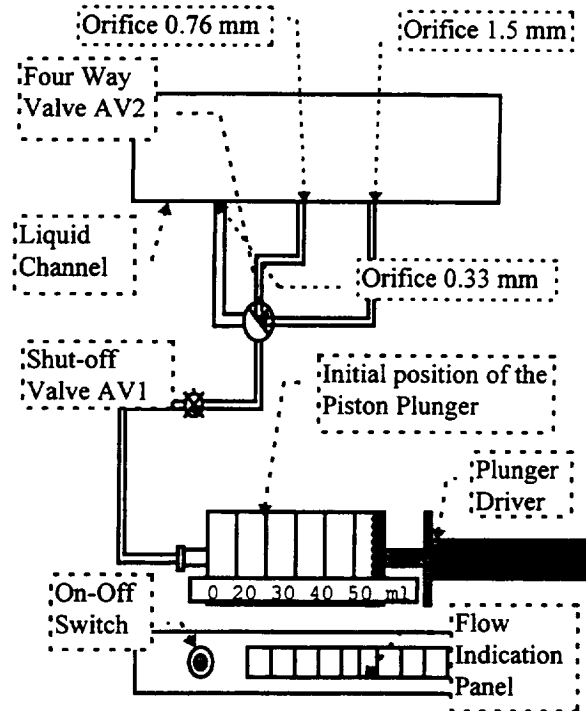
Figure 3. Low gravity flight configuration on board of the DC-9 low gravity platform.
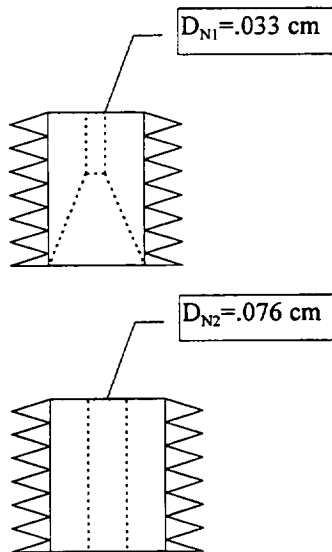
$D_{N1}=.033$ cm

$D_{N2}=.076$ cm

Figure 2. Schematic of air orifice design. The upper is an orifice with a converging nozzle design. The lower is a tubular design.
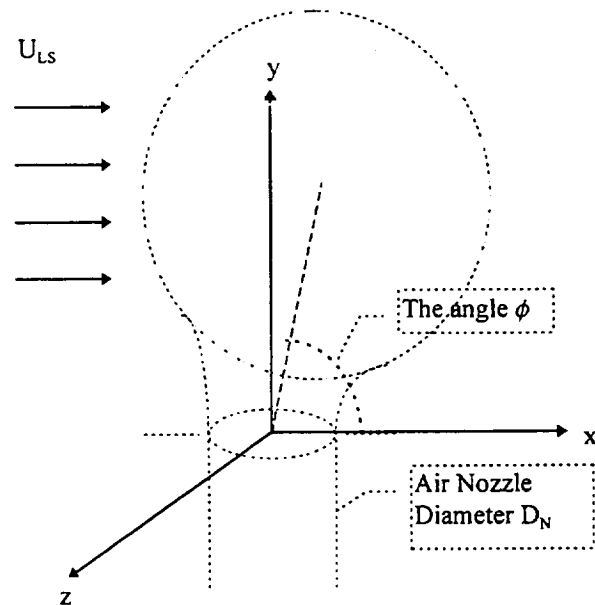
Figure 4. Coordinates and geometry of the Bubble Formation and Detachment in Liquid Cross Flow experiment. U_{LS} is in the + x axis and g in the - y axis.
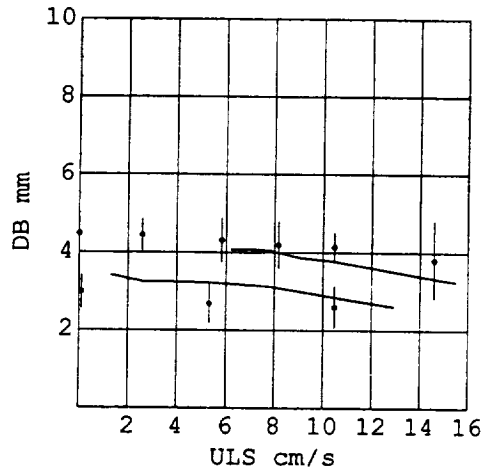
Figure 5. Experimental and predicted detachment diameter results for full g. The upper set of data and the continuous curve correspond to $D_N=.076$ cm. The lower set corresponds to $D_N=.033$ cm.
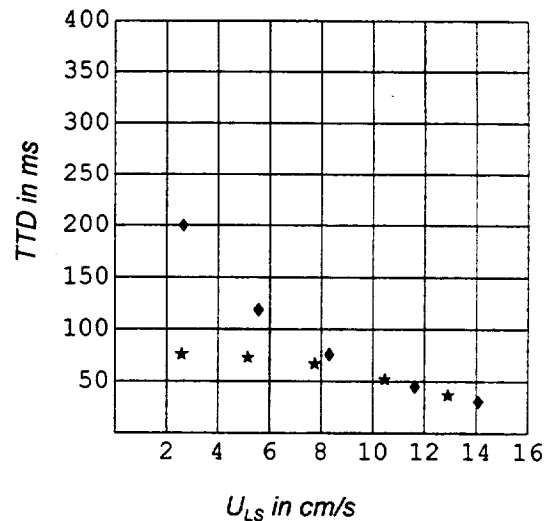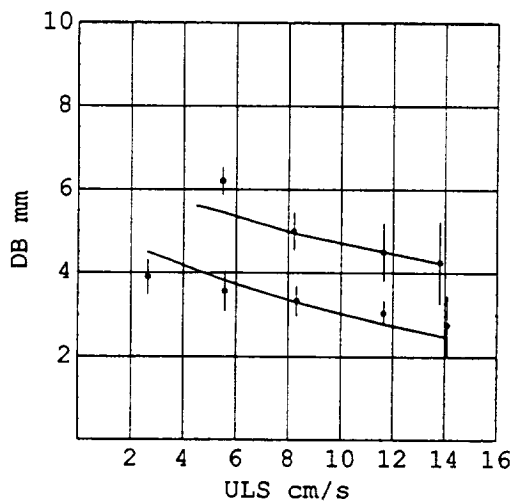

Figure 7. Predicted TTD in ms as a function of U_{Ls} for full g ($\star$) and low g ($\blacklozenge$) and for $D_N=.033$ cm. Q_d in this case is 8 ml/min. The higher curve at small U_{Ls} corresponds to the low g predicted TTD.

Figure 6. Experimental and predicted detachment diameter results for low g. The upper set of data and the continuous curve correspond to $D_N=.076$ cm. The lower set corresponds to $D_N=.033$ cm.
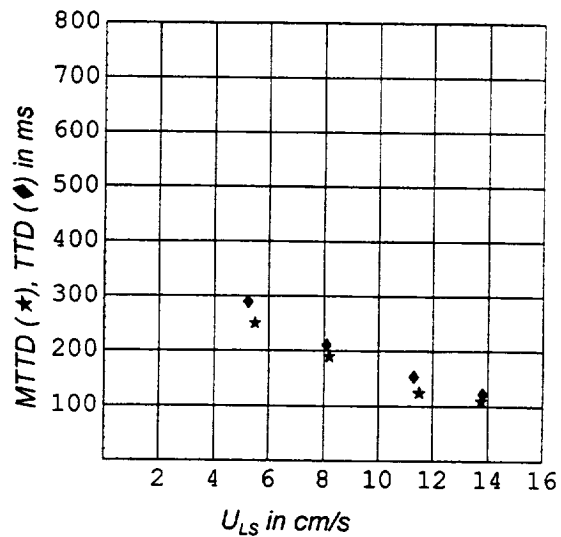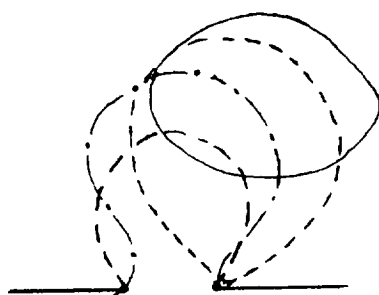

Figure 8. Experimental $MTTD$ ($\star$) and predicted TTD ($\blacklozenge$) in ms as a function of the cross liquid velocity for low g. $Q_d=3.8$ ml/min, $D_N=.076$ cm

a) 1 g

------------ 4 ms

--·--·--·--·--·-- 8 ms

················· 10 ms

————————— 12 ms
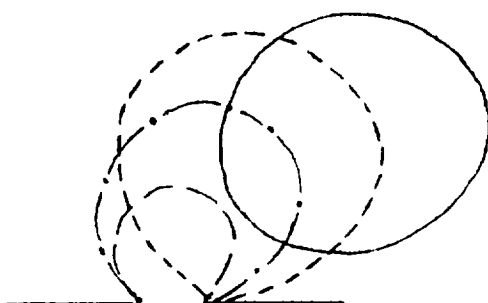
b) Low g

------------ 4 ms

--·--·--·--·--·-- 12 ms

················· 40 ms

————————— 48 ms

Figure 9. Comparison of bubble growth and detachment under 1 g (a) and in low g (b). Q_c=4000 ml/min, D_N=.033 cm, Q_d=10 ml/min.

REPORT DOCUMENTATION PAGE

Public reporting burden for this collection of information is estimated to average 1 hour per response, including the time for reviewing instructions, searching existing data sources, gathering and maintaining the data needed, and completing and reviewing the collection of information. Send comments regarding this burden estimate or any other aspect of this collection of information, including suggestions for reducing this burden, to Washington Headquarters Services, Directorate for Information Operations and Reports, 1215 Jefferson Davis Highway, Suite 1204, Arlington, VA 22202-4302, and to the Office of Management and Budget, Paperwork Reduction Project (0704-0188), Washington, DC 20503.

1. AGENCY USE ONLY (Leave blank)	2. REPORT DATE	3. REPORT TYPE AND DATES COVERED
	January 1998	Technical Memorandum

4. TITLE AND SUBTITLE

Bubble Formation and Detachment in Liquid Flow Under Normal and Reduced Gravity

5. FUNDING NUMBERS

WU–962–24–00–00

6. AUTHOR(S)

Henry K. Nahra and Y. Kamotani

7. PERFORMING ORGANIZATION NAME(S) AND ADDRESS(ES)

National Aeronautics and Space Administration
Lewis Research Center
Cleveland, Ohio 44135–3191

8. PERFORMING ORGANIZATION REPORT NUMBER

E–11034

9. SPONSORING/MONITORING AGENCY NAME(S) AND ADDRESS(ES)

National Aeronautics and Space Administration
Washington, DC 20546–0001

10. SPONSORING/MONITORING AGENCY REPORT NUMBER

NASA TM—1998-206614
AIAA–98–0732

11. SUPPLEMENTARY NOTES

12a. DISTRIBUTION/AVAILABILITY STATEMENT

Unclassified - Unlimited
Subject Category: 34   Distribution: Nonstandard

This publication is available from the NASA Center for AeroSpace Information, (301) 621–0390.

12b. DISTRIBUTION CODE

13. ABSTRACT (Maximum 200 words)

Two-phase flows are present in a wide variety of applications for spacecraft thermal control systems design. Bubble formation and detachment is an integral part of the two-phase flow science. The authors objective is to experimentally investigate the effects of liquid cross velocity, gas velocity, and nozzle diameter on the bubble diameter at detachment under reduced and normal gravity and under relatively low gas flow rates. Results from ground (1 g) and reduced gravity experiments will be presented in this paper. For the 1 g experiment, a flow loop was designed and built to accommodate a range of liquid and gas flow rates. The reduced gravity experiment was conducted on the NASA DC-9 reduced gravity platform using the two-phase flow loop qualified for operation on the low-gravity platform. Flow visualization is accomplished using a high speed 500 frames/s camera. The results suggest that the existence of buoyancy force contributes to the faster detachment of bubbles. Buoyancy helps the detachment process which results in smaller bubbles being formed. In reduced gravity, although drag force is present, the virtual non-existence of buoyant force results in larger bubbles and longer times for detachment. Theoretical predictions are also presented in this paper and seem to agree with the experimental results.

14. SUBJECT TERMS

Bubble; Formation; Detachment; Liquid crossflow; Buoyancy; Drag; Liquid velocity; Microgravity; Two-phase flow

15. NUMBER OF PAGES

13

16. PRICE CODE

A03

17. SECURITY CLASSIFICATION OF REPORT	18. SECURITY CLASSIFICATION OF THIS PAGE	19. SECURITY CLASSIFICATION OF ABSTRACT	20. LIMITATION OF ABSTRACT
Unclassified	Unclassified	Unclassified	

NSN 7540-01-280-5500